

## The Earth's Free Oscillations

Large earthquakes cause low-frequency vibrations which give new information about the earth's interior.

Gordon J. F. MacDonald

The great Chilean earthquake of 22 May 1960 excited the earth's free modes of vibration, and these were observed for the first time. The detection of the free modes broadens the spectrum over which a geophysicist may look into the earth's dark interior. Prior to 1960, almost all information regarding the earth's interior had been derived from detailed investigations of times of arrival of elastic-body waves as recorded by seismographs. The elastic-body waves travel different paths through the earth and contain most of their energy in the high-frequency part of the spectrum (10 to 0.1 cy/sec). The interpretation of arrival times is based on a ray theory similar to the ray theory of geometrical optics. The use of low-frequency normal modes as a tool for the investigation of the earth is thus somewhat analogous to the astronomer's use of radio frequencies as a supplement to observations in the visual range.

### Free Vibrations of an Elastic Sphere

The observation and interpretation of the free oscillations is the latest chapter in an investigation begun in 1882 by the noted mathematical physicist Horace Lamb. If an elastic solid is tapped by a hammer, the elastic disturbance is initially carried outward by two traveling waves. The fast wave (*P* wave) carries with it the compression and rarefaction of ordinary sound. The slow

wave (*S* or shear wave) transmits particle motion at right angles to the direction of propagation. If the solid is sufficiently isolated from the surroundings, reflections from boundaries may set up standing waves. The solid then rings or vibrates at the normal mode frequencies. Lamb (*1*) showed that the free vibrations of an elastic sphere can be classified into two groups: The *toroidal* or torsional oscillations are those in which a particle executes motion on a spherical surface; there is no radial component of motion. The toroidal oscillations unite to form the familiar horizontally polarized shear waves ( $S_{II}$  waves) of classical seismology. The *spheroidal* oscillations combine both radial and tangential motion to produce compression and rarefaction. A degenerate spheroidal oscillation involves only radial motion; the entire sphere expands and contracts.

The notation adopted to describe the earth's free oscillations is similar in many ways to the notation used in atomic spectroscopy, thus reflecting the common mathematical structure of these two fields. The solution to the equations of motion of an elastic sphere can be separated into a function dependent upon radius and a function dependent on the angular coordinates. The angular function is written as a sum of surface spherical harmonics

$$X_l^m = P_l^m(\sin \theta) e^{i m \phi} \quad (1)$$

$P_l^m$  is the associated Legendre function. If we use a geographical coordinate sys-

tem,  $\phi$  is the longitude and  $\theta$  is the latitude. The time dependence can be included in the exponential as  $\exp [i(m\phi - \omega t)]$ , where  $\omega$  is the angular frequency. This represents a wave traveling with a speed of  $m/\omega$  radians per second. If  $m$  is positive, the wave travels from west to east; if  $m$  is negative, it travels from east to west. The two signs of  $m$  are symmetrical in a stationary sphere. Rotation destroys the symmetry and creates important differences between waves traveling from west to east and waves traveling from east to west. The numbers  $m$  and  $l$  are familiar in quantum mechanics as the magnetic and azimuthal quantum numbers, respectively;  $l$  and  $m$  must assume integral values, and these integers determine the surface pattern of deformation associated with a particular free oscillation. The number of lines of vanishing displacement associated with the angular coordinate  $\theta$  is  $l - |m|$ ; the number of nodal lines associated with the angular coordinate  $\phi$  is  $m$ . There will also be surfaces of zero particle displacement associated with the radial function.

Free oscillations can thus be characterized by three integers;  $l$  and  $m$  determine the pattern of displacement on the spherical surface, and  $n$  determines the number of internal nodal surfaces. The notation that has been adopted is  ${}_n S_l^m$ ,  ${}_n T_l^m$  for spheroidal and toroidal oscillation, respectively. The expression  ${}_n T_l^m$  denotes a toroidal oscillation with  $n$  radial nodal surfaces and a displacement pattern on the surface of the sphere fixed by the surface spherical harmonic with ordinal numbers  $l$  and  $m$ . In the  ${}_n S_2$  oscillation, a sphere alternately assumes a prolate and an oblate form; this is sometimes termed the football mode. In the  ${}_n T_2$  oscillation, one hemisphere differential rotates or twists relative to the other.

Lamb treated a homogeneous uniform sphere. It was recognized by Jeans that

The author, who was until recently affiliated with the Theoretical Division of the Goddard Space Flight Center, National Aeronautics and Space Administration, Washington, D.C., is now a member of the staff of the Institute of Geophysics and Planetary Physics, University of California, Los Angeles.

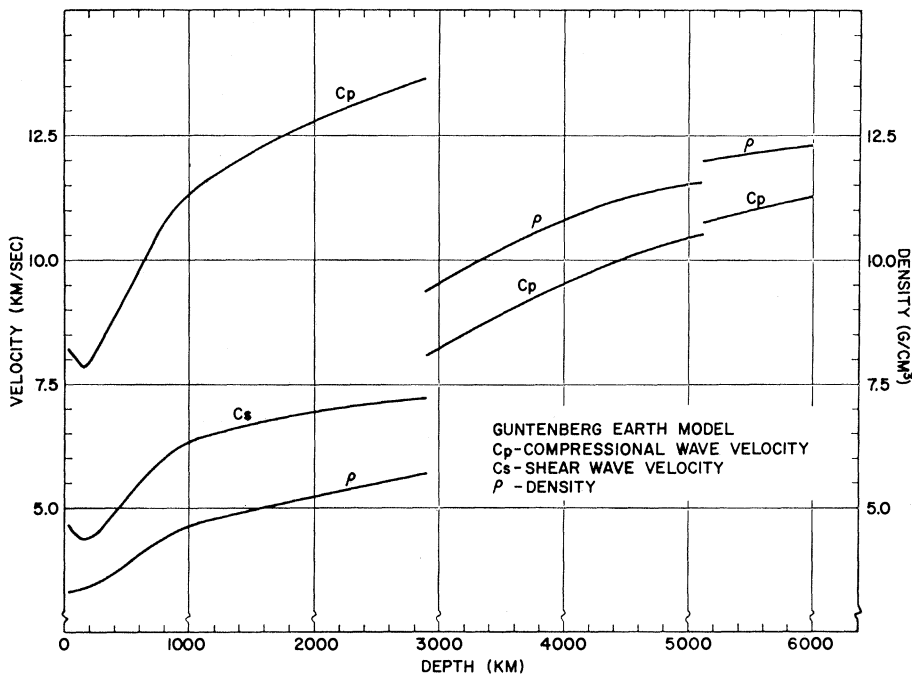


Fig. 1. The variation of the compressional- and shear-wave velocity and density within the earth. [According to Gutenberg (6)]

gravity influences the spheroidal oscillations, since these involve radial motion. At low frequencies, the gravitational forces are of the same order of magnitude as forces produced by elastic distortion; indeed it can be shown that over large regions of the earth there is a delicate balance between the two forces. A method of treating gravitational effects was suggested by Rayleigh (2) and was later employed by Love (3) and Jeans (4).

The solution to the problem of gravity failed to remove all difficulties in computing the periods of the free oscillations. The earth is inhomogeneous; the density and elastic properties vary in a radial direction. It is now known that the inner half of the earth contains a liquid core with a small inner core that is thought to be solid.

The reduction of observations of numerous earthquakes at many stations leads to estimates of the variation of

the *P*- and *S*-wave velocity. These velocities can be combined with the moment of inertia and mass of the earth to obtain an estimate of the variation of density within the earth (5). One such model of the earth's interior was constructed by Gutenberg (6, 7) (see Fig. 1). The characteristic feature of the Gutenberg model is a dip in the seismic velocities, beginning at the crust-mantle boundary and extending to a depth of 150 kilometers. Alternative models have been constructed by Bullen and Jeffreys (5). In these models the seismic velocities monotonically increase with depth; there is no region of low velocity (see Fig. 2). A particular model suggested by Bullen (Bullen model B) contains an inner core of much higher density (17.9 g/cm<sup>3</sup>) than that postulated in the Gutenberg model.

The extension of the theory for a homogeneous sphere to an inhomogeneous earth involves formidable computational problems. Stoneley, in 1926 (8), suggested a variational method, and much of the work since that date has been based on this approach. Pekeris and his coworkers proposed direct numerical methods, and these methods made possible a massive computational effort in which electronic computing machines were employed (9-11).

The effects of the inhomogeneous elasticity and density on the free oscillations are illustrated in Figs. 3 and 4, where the Gutenberg-model earth is contrasted with a homogeneous model in which the elasticity equals the aver-

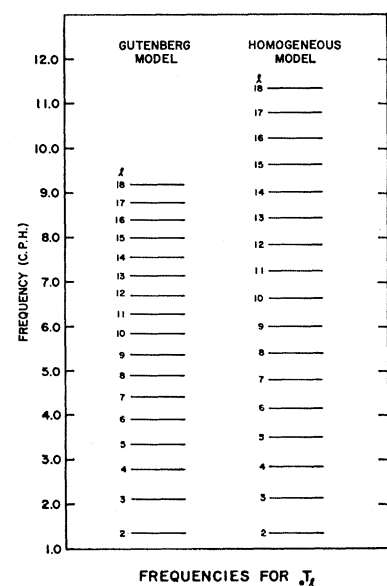
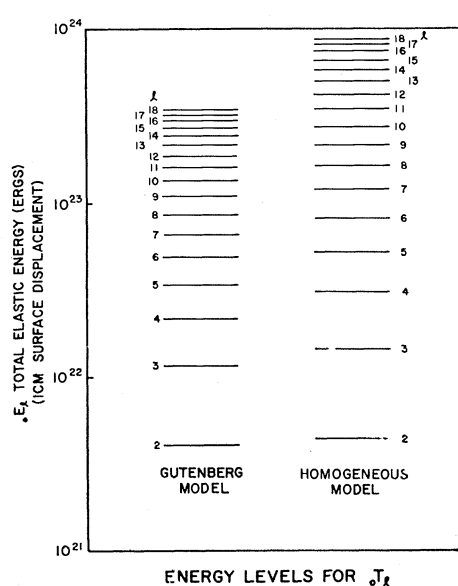
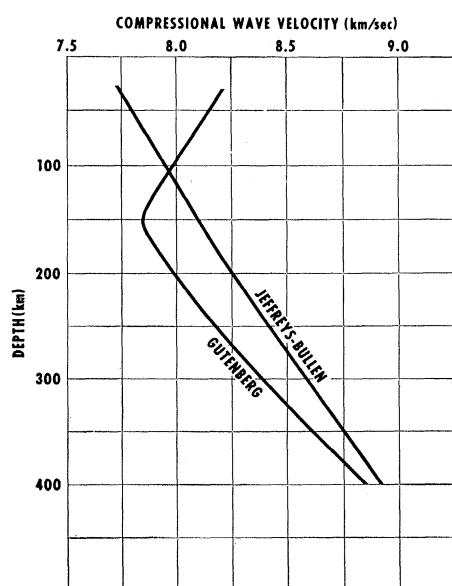


Fig. 2 (left). Comparison of the Gutenberg and the Bullen models in the upper mantle. Fig. 3 (middle). Total elastic energy in the fundamental toroidal oscillation. The energy is normalized to a 1-centimeter surface displacement. Fig. 4 (right). Comparison of resonant frequencies for the toroidal oscillations in the Gutenberg and the homogeneous models. [Figs. 3 and 4, after MacDonald and Ness (10)]

Fig. 5 (top). Total elastic energy per unit radius in the toroidal oscillations for the Gutenberg model. [After MacDonald and Ness (10)]. Fig. 6 (middle). Power spectrum of the gravity record after the Chilean earthquake of 22 May 1960. University of California (Los Angeles) earth-tide gravimeter; recording period, 23–27 May; 110-hour record; interval, 1 minute; sensitivity, 0.1  $\mu$ gal. [After Ness, Harrison, and Slichter (17)]. Fig. 7 (bottom). Power spectrum of the quiet period one month after the Chilean earthquake. University of California (Los Angeles) earth-tide gravimeter; recording period, 23–28 June; 116-hour record; interval, 1 minute; sensitivity, 0.1  $\mu$ gal. [After Ness, Harrison, and Slichter (17)]

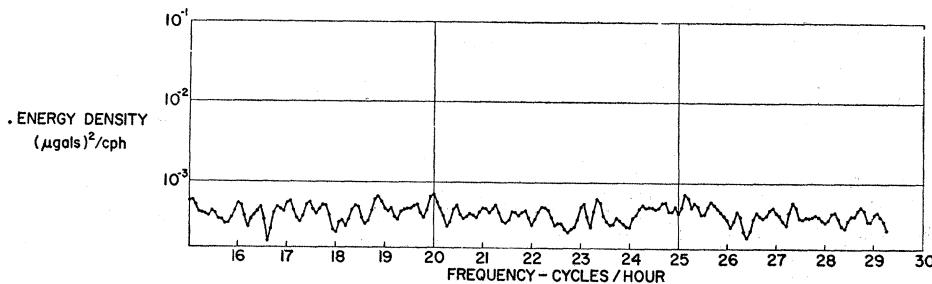
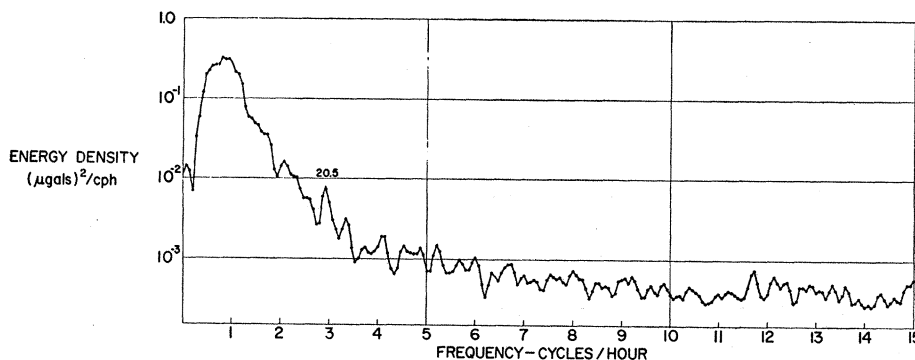
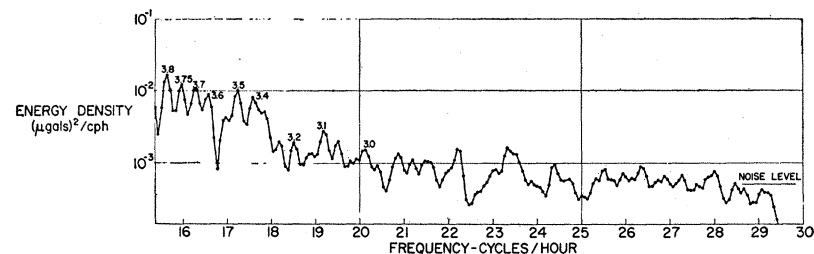
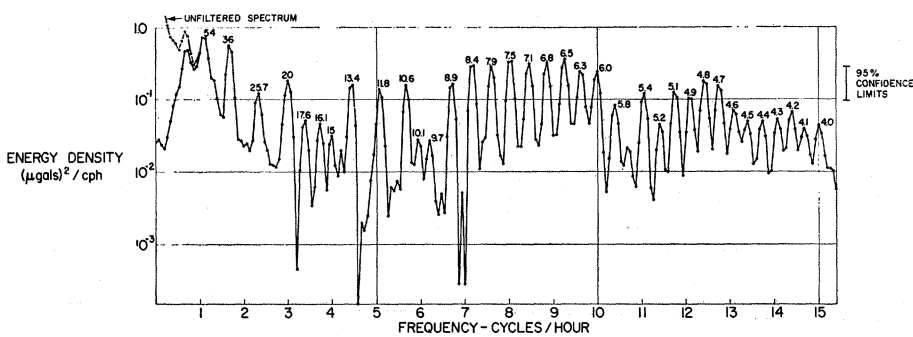
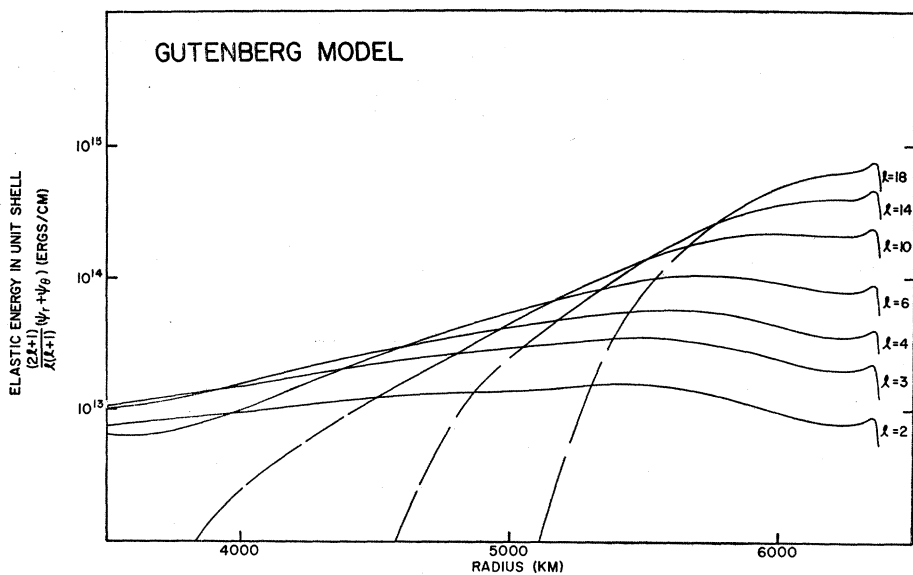
age elasticity of the Gutenberg model. The energy levels shown in Fig. 3 are normalized to provide a 1-centimeter displacement at the surface. About  $3 \times 10^{21}$  ergs are required to produce this displacement, with a  $\sigma T_2$  surface pattern in both the homogeneous and the inhomogeneous models. At higher modes and higher frequencies (Fig. 4) it takes more energy to form the more complicated surface pattern of displacement while maintaining a maximum surface amplitude of 1 centimeter. The needed energy is greater in the homogeneous model, since the near-surface rigidity is larger than in the Gutenberg model. The difference increases with increasing value of the mode number  $l$ .

The energy is more or less evenly distributed over the entire mantle at low mode numbers (see Fig. 5). At higher mode numbers the elastic energy is concentrated in the outer layers of the mantle. The  $\sigma T_2$  oscillation involves the mantle; the  $\sigma T_{18}$  oscillation is confined to the upper few hundred kilometers.

A further development in the theory should be noted. Jeans (4) showed that the free oscillations excited by an earthquake could be regarded as a system of dispersive surface waves and other waves diffusing into the earth's interior. Jeans established the correspondence of normal mode theory and ray theory in an elegant way. The ray-wave theory emphasizes the high-frequency part of the spectrum; the normal mode theory, the low frequencies.

### Observation of the Earth's Free Oscillations

Despite the considerable theoretical efforts, only recently was an attempt made to observe the earth's oscillations. Benioff constructed a strain-measuring



seismometer in the form of a silica glass rod 24 meters long, with the particular purpose of investigating the low-frequency spectrum. Benioff suggested that an apparent 57-minute periodicity visible on the strain records of the Kamchatka earthquake of 1952 was the  $s_2$  mode. This single suggestion of Benioff's prompted extensive computational work.

A second attempt at detecting the free oscillations was made in 1958, by spectrally analyzing the background noise in the strain seismometer and in the changes of the local gravitational field (12). Between 1958 and 1960 several instrumental developments made possible the observation of the free oscillations excited by the Chilean earthquake. Benioff, at the Seismological Laboratory of the California Institute of Technology, modified the circuitry associated with the strain seismometer so that the effect of the finite-amplitude earth tides was reduced and a greater magnification was achieved. A lower noise level was achieved on the LaCoste-Romberg gravimeter operated by the Institute of Geophysics at the University of California (Los Angeles). In addition, the Lamont Geological Observatory installed a strain gauge of the Benioff type in a mine shaft near Ogdensburg, New Jersey.

The free oscillations excited by the Chilean earthquake were detected on both the gravimeter and the strain seismometer. The instruments complement each other. The strain seismometer is sensitive to strain produced both by vertical and by horizontal motion; it therefore records both spheroidal and toroidal oscillations. On the other hand, the gravimeter records only vertical accelerations and spheroidal oscillations. A combination of the observations from the two instruments permits separation and identification of the two classes of motion.

The power spectrum of the variations in gravity at Los Angeles for the 4 days following the Chilean earthquake is shown in Fig. 6. Figure 6 should be compared with Fig. 7, a record of a quiet interval of 116 hours 1 month after the earthquake. This spectrum is almost structureless, though there is a peak at 20.5 minutes.

The spectrum of a seismic disturbance is thus characterized by well-defined sharp peaks for periods that vary between 1 hour and about 8 minutes. At higher frequencies the isolated peaks begin to merge into a continuum as a result of the finite width of an in-

Table 1. Comparison of calculated and observed toroidal oscillations (in minutes).

Order	Calculated			Observed
	Bullen B	Gutenberg	Gutenberg IV	
2	44.18	43.63	44.11	42.94
3	28.62	28.25	28.55	28.57
4	21.92	21.64	21.86	21.95
5	18.09	17.86	18.04	18.02
6	15.55	15.37	15.52	15.51
7	13.72	13.60	13.72	13.75
8	12.33	12.24	12.35	12.35
9	11.23	11.17	11.26	11.24
10	10.35	10.29	10.38	10.33
11	9.59	9.56	9.64	9.614
12	8.95	8.94	9.01	9.065
14	7.92	7.93	7.99	7.985

dividual peak and the increased number of peaks. Similar observations and analyses of the resulting data were carried out on records of strain by Benioff, Press, and Smith (13, 14) and by Alsop, Sutton, and Ewing (15).

#### Determination of Earth Models

A comparison between the spheroidal modes calculated by Peckeris, Alterman, and Jarosch (16) and those measured by Ness, Harrison, and Slichter (17) is shown in Fig. 8. At low frequencies the observations favor neither model, but at higher frequencies the observations closely fit the Gutenberg model.

Table 1 gives a comparison between the calculated and the observed toroidal oscillations. In addition to data for the Gutenberg model shown in Fig. 1, data for a modified Gutenberg model, Guten-

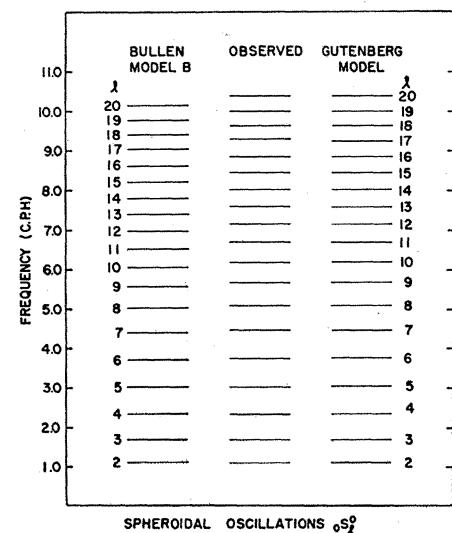


Fig. 8. Comparison of the calculated and the observed frequencies of the spheroidal oscillations.

berg IV, are included. The observed periods are consistently shorter than those of the Gutenberg model in the low-order oscillations, and the periods are more nearly equal in the high-order oscillations. This suggests that, on the average, the Gutenberg model has too high a rigidity. The perturbation of the Gutenberg model to form Gutenberg IV is controlled by the fact that the low-order oscillations involve the entire mantle of the earth while the higher-order oscillations reflect the properties of only the outer few hundred kilometers. The Gutenberg IV model is produced by reducing the shear-wave velocity throughout the lower part of the mantle by 2 percent and maintaining the Gutenberg velocity distribution in the outer 400 kilometers.

Comparison of the toroidal and spheroidal oscillations with models of the earth strongly indicates a preference for a model with a region of low velocity. This provides additional supporting evidence for the existence of a region of low velocity (18).

In the Gutenberg model the velocity increases everywhere in the mantle but in a thin, near-surface region. The conditions which give rise to the anomalous decreasing velocity are of great interest. Laboratory measurements show that in silicates the wave velocity increases with increasing pressure; pressure stiffens a rock. An increase in temperature has the opposite effect, decreasing the wave velocity. In the outer regions of the earth, both pressure and temperature increase; the velocity decreases if the increase in temperature wins out over the increase in pressure. An extrapolation of laboratory data indicates that a gradient of 6 to 7 degrees per kilometer is sufficient to produce a decrease in velocity (10, 19). One can then inquire as to what distributions of radioactive heat sources and thermal conductivity are sufficient to give the required critical temperature gradient and at the same time account for the heat flowing from the earth's interior.

It is generally assumed that the radioactive heat sources are concentrated toward the surface. The concentration is greater under continents than under oceans. The thermal conductivity may vary because of the contribution of radiation at high temperatures. The combination of the near-surface concentration of heat sources and a thermal conductivity increasing with depth requires that the steepest temperature gradient exist in the upper mantle. If the low-velocity zone is in-

deed caused by a high temperature gradient, then the low-velocity zone should begin at the base of the crust rather than at some greater depth (100 to 200 kilometers), as has been suggested on the basis of studies of nearby earthquakes.

The thermal conditions that could give rise to the low-velocity zone are illustrated in Figs. 9 and 10. Conditions approximating the upper mantle under oceans are shown in Fig. 9. The radioactivity is concentrated in the upper 430 kilometers, and there is no further concentration of radioactivity near the surface. The calculated temperature gradient exceeds the gradient required to produce a low-velocity zone at depths ranging from 100 to 150 kilometers. Figure 10 illustrates the conditions that might be expected under continents. The radioactivity is distributed over the upper 430 kilometers, but half of it is placed above 30 kilometers. The near-surface concentration of radioactivity reduces the temperature gradient, and a low-velocity zone exists at depths down to 50 to 100 kilometers. The calculations suggest that there should be a marked difference in the extent of the low-velocity zone under continents and oceans. The low-velocity zone should extend to greater depths and be better developed under ocean areas.

The low-velocity zone might be due to large-scale chemical inhomogeneity in the upper mantle. According to this hypothesis, the low-velocity zone could be found at greater depths. Detailed studies of surface waves and artificial explosions are needed for an understanding of the origin of the low-velocity layer.

### Earthquake Energy

Estimates of the energy released during a large earthquake differ by factors of 10. A source of uncertainty is the energy contained in the low-frequency end of the spectrum. The energy levels of the toroidal oscillation shown in Figs. 3 and 4 can be combined with observations on particle displacement at the surface to yield an estimate of the energy in the earthquake at these low frequencies. The displacement obtained by the strain seismometers in the Chilean earthquake give an energy density in the  $T_2$  mode of  $5 \times 10^{18}$  ergs per cycle per hour. The total energy in the toroidal oscillations that have a period greater than 9 minutes is about  $10^{20}$  ergs. If there is equipartition of

energy between the toroidal and the spheroidal oscillations, then about  $10^{21}$  to  $10^{22}$  ergs of energy were initially present in oscillations with periods greater than 1 minute. These figures should be compared with the  $10^{24}$  ergs estimated for total elastic energy released by the Chilean earthquake.

### Line Structure

Ness (17) and Smith (13), in reducing the data from the Chilean earthquake, noted that the low-frequency spectral peaks appeared as doublets or triplets instead of single lines as would be expected for a stationary elastic sphere (11). Rotation destroys the symmetry with respect to the integer  $m$  in Eq. 1, and the degeneracy associated with the symmetry is removed. The effect of rotation on the oscillations can be qualitatively understood by recalling that a free oscillation is composed of a number of running waves. Waves traveling in the direction of the earth's rotation are carried forward relative to waves traveling in the opposite direction. The net effect is that the total pattern of surface deformation rotates relative to the earth. The local effect is to cause the vibrating particles to precess, much in the manner of a Foucault pendulum. The rotational splitting is analogous to the Zeeman effect in spectroscopy, where a magnetic field removes the degeneracy with respect to the quantum number  $m$ . Detailed calculations of the splitting in spheroidal and toroidal oscillations have been made (10, 20). The calculated splitting is in agreement with the splitting observed in the low-order spheroidal oscillations, an oscillation of order  $l$  being split into  $2l + 1$  peaks. The fine structure of the lowest-order toroidal oscillation is in doubt and the line  $T_2$  presents a number of problems. It should be remarked that rotational splitting of the elastic vibrations is analogous to the effect of rotation on the axisymmetric oscillations of a fluid sphere. These oscillations have been studied in detail by astrophysicists concerned with variable stars. Indeed, Cowling and Newing (21) obtained an expression for the rotational frequency shift in the free oscillations of a star that is identical in form to that describing the effect of rotation on the elastic vibrations of the earth.

If the earth were a perfectly elastic body, then the spectral peaks should show up as individual lines broadened

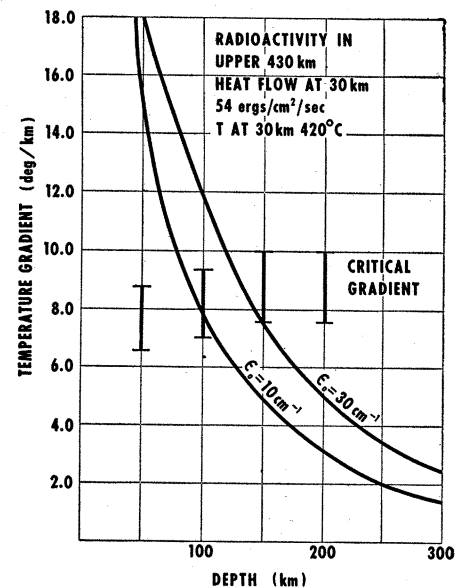


Fig. 9. Computed thermal gradient under a typical ocean. The critical temperature gradient required to produce a low-velocity zone is indicated by the heavy vertical lines.

only by the data-reduction techniques (instrumental broadening). The deviations from perfect elasticity or fluidity results in a natural broadening of the lines. The degree to which a given line is broadened, or, alternatively, the rate at which a given peak decays, provides, in time, a measure of the anelastic properties of the earth.

The distribution of the anelastic properties can be obtained by studying

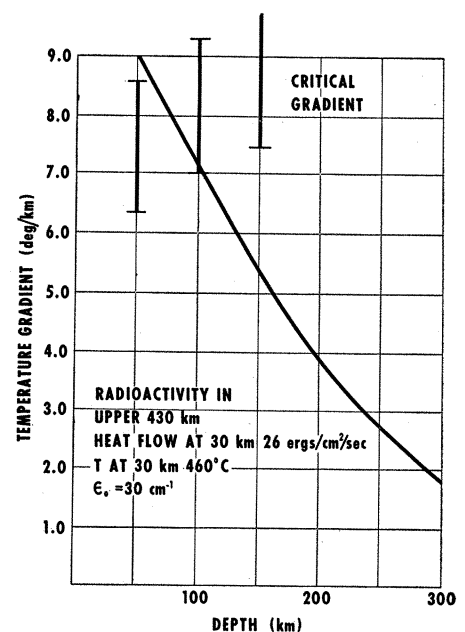


Fig. 10. Computed thermal gradient under a typical continental region. The critical temperature gradient required to produce a low-velocity zone is indicated by the heavy vertical lines.

the decay rate of oscillations of various frequencies, since differing frequencies represent different portions of the earth. Furthermore, several mechanisms of dissipation will be prominent in the various oscillations. The spheroidal oscillation of order 2 involves the entire earth, including the core, and the motion contains components of compression and shear. The radial oscillation  $s_0$  involves only compressional motion, and this oscillation provides a measure of the dissipation of the earth in compression. The broadening of the toroidal lines is due primarily to dissipative processes within the mantle. The interaction of the core and mantle provides an additional sink of energy. A detailed study of possible viscous and hydromagnetic effects rules out the core-mantle boundary as a major contributor to the energy loss (10).

The half width of the lines,  $Q$ , or the rate of energy dissipated per cycle per peak elastic energy is found to be about 350 for spheroidal oscillations. Thus, in spheroidal oscillation the earth rings as a rather poor bell. The estimates of the  $Q$  for toroidal oscillations are less good, but somewhat lower figures are indicated. The highest  $Q$  of all is shown by the radial oscillation. As may be noted in Figs. 1 and 2, the earth appears to be ringing in this mode of oscillation a month after the earthquake. The indicated  $Q$  is greater than 1000. The dissipation in compression is thus much less than in shear. Such a conclusion is in agreement with the suggestion by Knopoff and MacDonald (22) that the major mechanism for dissipation of small-amplitude waves in the earth is frictional rubbing across grain boundaries.

### Core Problems

Smith (23), in a careful analysis, finds that the period of the fundamental toroidal oscillation is 42.94 minutes. This period is more than a minute less

than the period predicted for the Gutenberg IV model, which gives a reasonable fit to the other oscillations. The deviation is in the direction one would expect if the core-mantle boundary were partly rigid; the resonant period for a mantle with a rigid inner surface is 32.1 minutes. A possible explanation of the apparent stiffness involves the earth's magnetic field. A component of the magnetic field tangential to the core-mantle boundary leaks out of the core into the conducting lower mantle. This component combines with the dipole component to give a Maxwell stress. The lower mantle is then partially glued to the core, and this leads to an apparent stiffness. If this interpretation is correct, an estimate can be made of the conductivity of the lower mantle and the strength of the magnetic field. Detailed studies of toroidal oscillations of low frequency may lead to fundamental information regarding the electromagnetic properties of the core and lower mantle.

Slichter (24) has emphasized the presence of a peak at the low-frequency end of the spectrum that is not theoretically predicted (see Fig. 1). A possible interpretation of this peak is that it represents the jiggling of the solid inner core, and that the jiggling is dampened by interaction with the fluid outer core. The problem remains open, however, since the reality of the peak remains to be established and the detailed dynamics of the inner-core oscillations remain to be explored.

### Conclusion

The development of sophisticated instrumentation has permitted investigation of the interior of the earth through use of a new frequency range. The results from a single earthquake have provided abundant new information regarding the earth's interior. Oscillations are excited only by large earthquakes. Over the period of the next

few years we may expect a few large earthquakes, and the associated vibrations will yield new knowledge on the internal constitution of our earth.

### References and Notes

1. H. Lamb, *Proc. London Math. Soc.* **13**, 189 (1882); an earlier investigation of the toroidal and radial vibrations of a homogeneous sphere was carried out by P. Jaerisch, *Crelle* **88**, 131 (1880).
2. Lord Rayleigh, *Proc. Roy. Soc. (London)* **A77**, 486 (1906); Rayleigh's method involves considering the strain as measured from the initially hydrostatically stressed state.
3. A. E. H. Love, *Some Problems of Geodynamics* (Cambridge Univ. Press, Cambridge, England, 1911).
4. J. H. Jeans, *Proc. Roy. Soc. (London)* **A102**, 554 (1923).
5. A clear and detailed discussion is given by K. E. Bullen, *An Introduction to the Theory of Seismology* (Cambridge Univ. Press, Cambridge, England, 1959).
6. B. Gutenberg, *Physics of the Earth's Interior* (Academic Press, New York, 1959).
7. J. Dorman, M. Ewing, J. Oliver, *Bull. Seismol. Soc. Am.* **50**, 87 (1960).
8. R. Stoneley, *Monthly Notices Roy. Astron. Soc. Geophys. Suppl.* **13**, 56 (1926).
9. Recent applications of the variational method have been made by N. Jobert, *Geophys. J.* **4**, 242 (1961), and H. Takeuchi, *ibid.* **4**, 259 (1961); the numerical techniques employed by Pekeris and his colleagues are described by Z. Alterman, H. Jarosch, and C. L. Pekeris, *Proc. Roy. Soc. (London)* **A252**, 80 (1959); alternative numerical schemes are discussed in 10 and 11.
10. G. J. F. MacDonald and N. F. Ness, *J. Geophys. Research* **66**, 1865 (1961).
11. F. Gilbert and G. J. F. MacDonald, *ibid.* **65**, 675 (1960); we suggested that the spectral lines would be split by the departure of the earth from sphericity and by the rotation.
12. H. Benioff, J. C. Harrison, L. LaCoste, W. H. Munk, L. B. Slichter, *J. Geophys. Research* **64**, 1334 (1959).
13. H. Benioff, F. Press, S. Smith, *ibid.* **66**, 605 (1961).
14. In 1960 Press reported to the American Geophysical Union the presence of higher-order free oscillations in seismic records of large earthquakes.
15. L. Alsop, G. Sutton, M. Ewing, *J. Geophys. Research* **66**, 631 (1961).
16. C. L. Pekeris, Z. Alterman, H. Jarosch, *Proc. Natl. Acad. Sci. U.S.* **47**, 91 (1961).
17. N. F. Ness, J. C. Harrison, L. B. Slichter, *J. Geophys. Research* **66**, 621 (1961).
18. F. Press, *Science* **133**, 1455 (1961).
19. F. Birch, *J. Geophys. Research* **57**, 227 (1952).
20. G. Backus and F. Gilbert, *Proc. Natl. Acad. Sci. U.S.* **47**, 362 (1961); C. L. Pekeris, Z. Alterman, H. Jarosch, *Phys. Rev.* **122**, 1692 (1961).
21. G. Cowling and R. A. Newing, *Astrophys. J.* **109**, 149 (1949).
22. L. Knopoff and G. J. F. MacDonald, *J. Geophys. Research* **65**, 2191 (1960).
23. S. Smith, thesis, California Institute of Technology (1961).
24. L. Slichter, *Proc. Natl. Acad. Sci. U.S.* **47**, 186 (1961).